Paper n° 022

A Qualitative Analysis of Vortex Ring State Entry Using a Fully Time Marching Unsteady Wake Model

Joëlle Bailly
joelle.zibi@onera.fr

Office National d'Etudes et de Recherches Aérospatiales
Applied Aerodynamics Department
8, rue des Vertugadins, 92190 Meudon, France

Introduction

The study of the behavior of helicopters during flights has shown the occurrence of a rather dangerous phenomenon, called the Vortex Ring State (VRS), during steep descent flights, when the helicopter is highly loaded. The consequences of this state can be delicate for the maneuverability of the helicopters. High levels of vibrations, drop of lift and inefficiency of the commands can lead to severe consequences. This dangerous flight regime was involved in different helicopter [1] and tilt-rotor crashes. The change of the collective pitch does not allow coming out this state (power-setting phenomenon). In general, the increase of the advancing velocity makes the helicopter get off this state, and the descent velocity is then getting stabilized. The Vortex Ring State is the first limiting regime in steep descent. This is why it is very important to understand its appearance, thanks to the analysis of flight [2] or wind-tunnel tests [3][4][5], and to be able to correctly predict it by numerical simulations.

The main objective of this study (performed in the framework of the PHIDIAS project, in cooperation with Eurocopter) is the validation of an unsteady wake model, developed in the MINT code by ONERA, on three configurations of entry into VRS, obtained during flight tests on the 6075 Dauphin, at the French flight test center, located in Istres. The MINT results will also be compared with the HOST comprehensive code results, obtained by using an induced velocity model adapted for steep descent cases, and in which a VRS criterion has been defined. The analysis of the MINT aerodynamic results will allow defining and checking some qualitative characteristics of the flowfield when the VRS phenomenon occurs.

Description of flight tests

In 2000 and 2001, ONERA performed flight tests campaigns on the 6075 Dauphin of Eurocopter, at the CEV French flight test center located in Istres [6]. During these tests, two procedures for the investigation of VRS have been evaluated:

- Decrease of the collective pitch from a level flight by trying to maintain a constant advancing velocity. The upper limit of the VRS domain can be determined by testing different values of advancing flights. The lower limit was then determined when the descent rate was stabilized;
- Deceleration of the helicopter, from a level flight with a rather high velocity while trying to maintain constant the descent rate. This allows determining the lateral limit of the VRS domain.

Figure 1 illustrates the experimental limits of the VRS domain of the 6075 Dauphin.

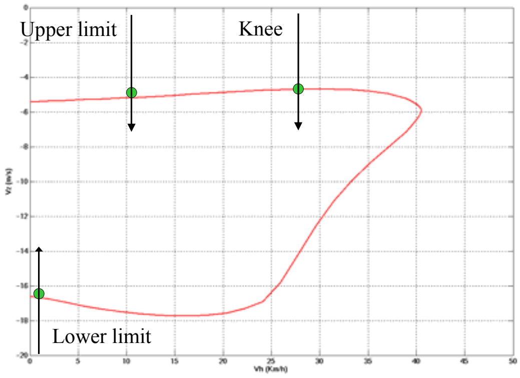

Figure 1: Experimental limits of the VRS domain of the 6075 Dauphin

For this study, three test points have been selected, corresponding to different procedures of entry into VRS:

- "upper limit": Vh=10km/h; Vz=-4.8m/s;
- "knee": Vh=28km/h, Vz=-4.50 m/s
- "lower limit": Vh=1km/h; Vz=-15.80m/s.

These points are represented in green in Figure 1.

Description of the numerical tools

Description of the HOST code

The HOST code [7], developed by Eurocopter, is an aeroelastic code used to compute the rotor trim, the aerodynamic performance and the vibration levels of the rotor. The aerodynamic modeling is based on the lifting line theory. At each azimuth, and for each section, an angle of attack and a sectional Mach number coefficient are computed and used to read aerodynamic coefficients in 2D polars. The wake model is computed by the METAR code which describes the vortex lattices by a prescribed helicoidal geometry. A coupling between HOST and METAR is made, until convergence is reached on induced velocities at the rotor disk level.

All the models of induced velocities available in the HOST code require the calculation of an average induced velocity term, determined in "classical" flight configurations (level flight, climb) by the momentum theory. But, for steep descent flights, the multiplicity of the solutions leads to numerical instabilities, and convergence problems. A semi-empirical approach, developed at ONERA [8], allows rectifying these problems. At the same time, the formulation of a VRS prediction criterion has been developed [8][9] based on the improvement of the Wolkovitch criterion [10], by taking into account the inclination angle of the wake. A too small value of the velocity of the release of the vortices can be considered as a responsible factor of the vortex ring state, the tip vortices being maintained in the vicinity of the rotor. The following semi-empirical criterion expresses the closeness of the helicopter to the VRS region:

$$\varepsilon = \sqrt{\left(\frac{V_h}{kV_{i0}}\right)^2 + \left(\frac{V_z}{V_{i0}} + \frac{V_i}{2V_{i0}}\right)^2}$$

where V_h is the horizontal advancing velocity, V_z the descent velocity, V_{i0} the mean induced velocity in hover, and V_i the mean induced velocity of the considered flight test. It has been shown that the values of the coefficients $\varepsilon=0.25$, and $k=4$ allow obtaining a very satisfying correlation with experimental domains (V_h,V_z) for different helicopters.

Description of the MINT code

The wake model MINT [11][12], developed at ONERA, is an efficient and accurate numerical tool which computes the unsteady wake of a helicopter rotor (initialized by both the METAR prescribed wake and the MESIR free-wake models), for stabilized but also for maneuver flight cases. The MINT code simulates the aerodynamics and the wake of a rotor, by a time marching method, using the general theory of the vortex sheets. The wake is modeled by a swirly potential discontinuity surface, discretized in panels of constant gradient of potential jump. This discretization improves the order of accuracy and the stability in comparison with the method using a discretization of the wake by lattices. Moreover, no regularization is used to compute the aerodynamic field. The numerical integration used to compute the velocities induced by the panels is performed with a 4-point Gauss method. The time marching scheme is a one-step Runge-Kutta scheme with sub-iterations to converge to the circulation on the blade, and the emission condition of the wake at each time step.

In the present study, the blades are supposed to be rigid in the HOST comprehensive dynamic code. The computations in both HOST and MESIR codes correspond to a succession of stabilized flights, performed with a progressive variation of the V_z descent velocity, for a given V_h advancing velocity. In order to find a compromise between an accurate simulation of the physical phenomena which occur during the VRS entry, and the cost of the CPU time of the MINT calculations, it has been chosen to keep 6 rotor revolutions in the wake, and to perform 60 rotor revolutions during each step of descent velocity. The temporal discretization is rather fine (5° per time step, which amounts to 72 iterations per rotor revolution). The MINT code has the advantage to require largely reduced CPU time (38 hours with the chosen numerical parameters on the Nec SX-8) in comparison with classical CFD codes [13] (up to several hundred hours on the Nec SX-8), and to be much less dissipative.

Analysis of the HOST results

HOST computations have been run using the induced velocities model modified for the steep descent flights. The VRS criterion is also evaluated. The evolutions of the collective pitch angle and the VRS criterion are plotted with respect to the vertical velocity Vz, for the three different advancing velocities corresponding to the three selected flight configurations (Figure 2).

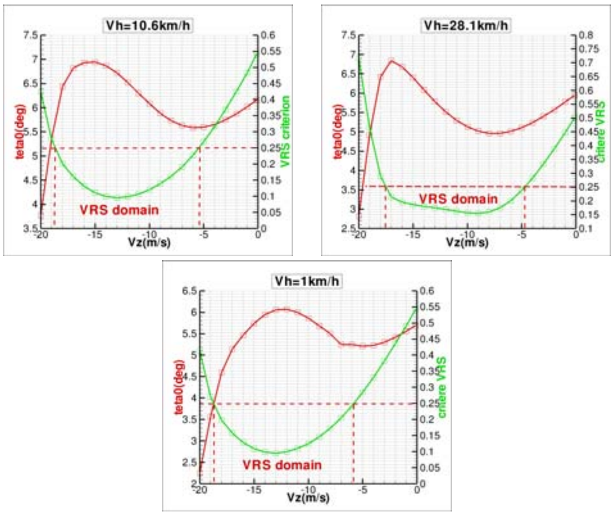

Figure 2: Evolutions of the collective pitch angle and the VRS criterion computed by HOST

The HOST computations provide the following couples of velocities (Vh,Vz) corresponding to the entry into VRS when the value of the VRS criterion is equal to 0.25:

- "upper limit": Vh=10.6km/h; Vz=-5.4m/s;
- "knee": Vh=28.1km/h; Vz=-4.7m/s;
- "lower limit": Vh=1km/h; Vz=-18.7m/s.

For the three test cases, the correlation with experiment of the theoretical values of the couple of velocities is very satisfactory for the two first cases, and slightly over-predicted for the "lower limit" configuration.

From the pure advancing flight (Vz=0m/s), the increase of the descent velocity leads to a decrease of the angle of the collective pitch, until a minimum value (which corresponds to the value of 0.25 of the VRS criterion defined in the HOST code). As it is observed during the flight tests, the increase of the collective pitch angle does not allow the exit from the VRS phenomenon, which appears for a rather high value of the descent rate (around -18m/s for Vh=10.6km/h, and Vh=1km/h, and around -17m/s for Vh=28.1km/h).

Analysis of the MINT results

Description of MINT calculations strategy

MINT calculations are performed for the given advancing selected test case, and the descent velocity is progressively varying from -0.1 to -7m/s, -0.1 to -6m/s, and -20 to -14m/s, each 1m/s, respectively for the three flight configurations (upper limit, knee and lower limit). In the following paragraphs, these three configurations will be always studied in this order.

Frequency analysis of the rotor loads

The evolutions of the components of the rotor loads (thrust Fz, drag Fx, and lateral force Fy) with respect to the number of MINT iterations are plotted for the three configurations respectively in Figure 3, Figure 4 and Figure 5.

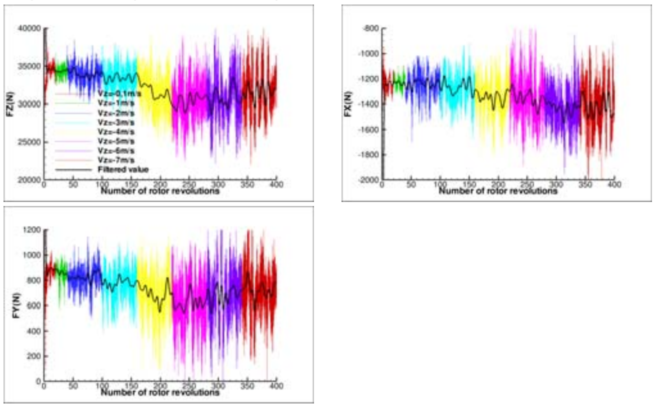

Figure 3: Rotor loads evolutions versus MINT iterations (Vh=10.6km/h)

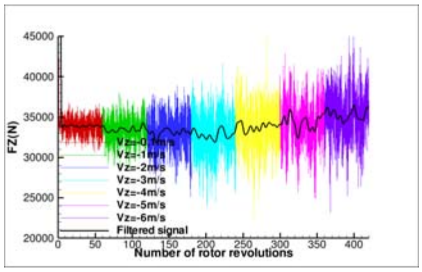

Figure 4: Rotor thrust evolution versus MINT iterations (Vh=28.1km/h)

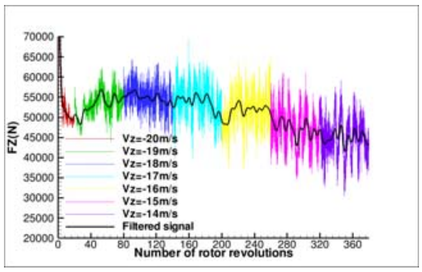

Figure 5: Rotor thrust evolution versus MINT iterations (Vh=1km/h)

For the "upper limit" configuration (Vh=10.6km/h), the mean value of the thrust computed with MINT is equal to 31000N (corresponding to a helicopter weight of 3160kg). This value is lower than the one computed with the HOST code, which is of 35540N (corresponding to a helicopter weight of 3625kg). This difference between these two evaluations of the thrust is due to the different aerodynamic model used in the codes. Moreover, the MINT calculations are not trimmed. This could be improved by coupling the two codes (validation in progress).

One of the criteria of the VRS entry is the occurrence of high amplitude of fluctuations of the rotor thrust. From Figure 3, these oscillations significantly increase from Vz=-4m/s. Such oscillations are also noticed for the drag and the lateral load from Vz=-4m/s. For the “knee” configuration (Figure 4), the increase of the fluctuations of the loads approximately happens from Vz=-3m/s. It is not so easy to determine this level with this criterion, the level of fluctuations of the loads being rather high from the lowest value of descent rate, and their variation being progressive. For the “lower limit” configuration (Figure 5), an increase of the fluctuations of the loads can be noticed from Vz=-18m/s.

Another criterion for the VRS entry is the appearance of low frequency load oscillations (which are felt during flight tests through an important level of vibrations). A frequency-time post-processing (using MATLAB software) is applied to determine the spectral power density of the loads computed by MINT, for each descent rate value, on which a numerical Hamming window is applied. The sampling frequency is calculated from the experimental value of the rotational speed, and the temporal discretization of the MINT calculations (5° per time step).

The evolution of the PSD of the rotor thrust versus the entire scale of frequency (left) and around the very low frequency (right) is represented for the three test cases, respectively in Figure 6, Figure 7 and Figure 8.

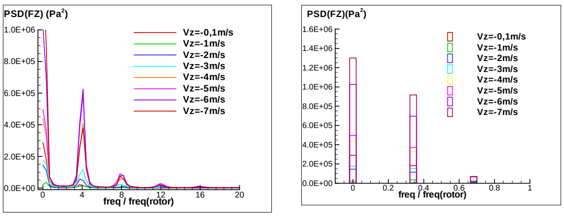

Figure 6: Evolution of the power spectral density of the thrust with respect to frequency (Vh=10.6 km/h)

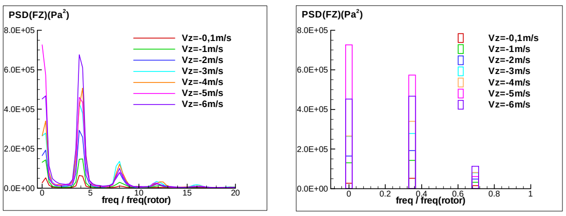

Figure 7: Evolution of the power spectral density of the thrust with respect to frequency (Vh=28.1km/h)

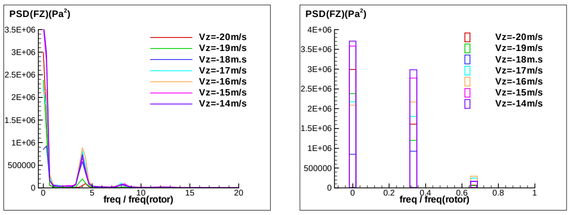

Figure 8: Evolution of the power spectral density of the thrust with respect to frequency (Vh=1km/h)

It can be noticed a continuous increase of the amplitude of the peak of the PSD of the rotor thrust around 4/rev and 8/rev (multiple of the frequency blade passage of the 4-bladed Dauphin 6075 helicopter) from Vz=0m/s to Vz=-5m/s for the upper limit configuration, until Vz=-4m/s for the knee configuration, and Vz=-18m/s for the lower limit configuration. Moreover, this frequency post-processing clearly shows the appearance of a very low frequency phenomenon when the descent rate is increased.

The evolution of the amplitude of the PSD of the rotor thrust versus the descent rate, at the very low frequency of 0.34/rev and around the 4/rev frequency are plotted respectively in Figure 9, Figure 10 and Figure 11 for each configuration. For the upper limit case, Figure 9 clearly shows the sudden increase of the energy of the considered signal between -3 and -4 m/s.

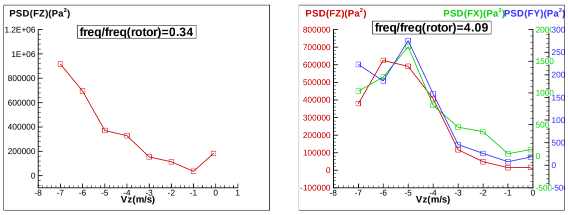

Figure 9: Evolution of the maximum amplitude of the PSD of the rotor loads versus the descent rate (Vh=10.6km/h)

For the “knee” test case (Figure 10), the accentuation of this increase can be seen at the very low frequency from Vz=-4m/s, while a first maximum value is obtained at Vz=-4m/s at the 4.17/rev frequency.

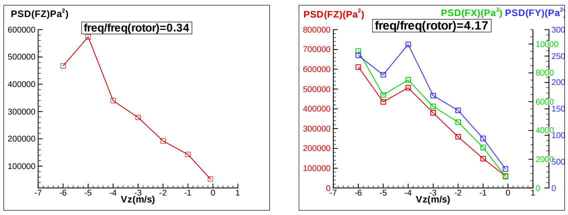

Figure 10: Evolution of the maximum amplitude of the PSD of the rotor loads versus the descent rate (Vh=28.1km/h)

Figure 11 clearly shows that a deep increase of the PSD of the thrust occurs from Vz=-18m/s for the very low frequency of 0.34/rev, and that the level of PSD reaches its maximum value from Vz=-17m/s for the 4/rev frequency.

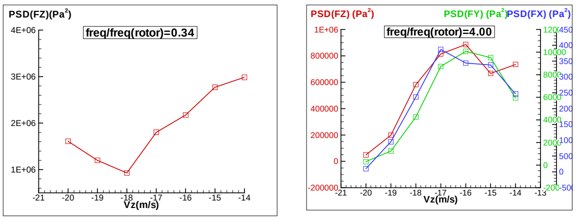

Figure 11: Evolution of the maximum amplitude of the PSD of the rotor loads versus the descent rate (Vh=1km/h)

This frequency analysis of the MINT results obtained for the three configurations clearly shows the sudden appearance of a very low frequency phenomenon, which can be identified as the entry into the vortex ring state regime.

<u>Aerodynamic analysis</u>

We will now focus on the analysis of the aerodynamic variables obtained with the MINT calculations.

<u>Sectional lift coefficient</u>

The radial evolutions of the sectional lift coefficient, for each of the 4 blades of the rotor (blade 1 at ψ=0°, blade 2 at ψ=90°, blade 3 at ψ=180°, blade 4 at ψ=270°), obtained during the last rotor revolution at each step of the descent rate, are plotted in Figure 12, Figure 13 and Figure 14 respectively for each flight case.

Concerning the upper limit configuration (Figure 12), for Vz=-2m/s, the lift coefficients of each blade present similar evolutions, the differences being due to the cyclic commands. From Vz=-3m/s, discrepancies begin to appear, especially at the tip of blade 3 (ψ=180°), and at the root of blade 1 (ψ=0°). For Vz=-4m/s, a drastic modification of the evolutions of the lift coefficient can be noticed between the four blades. The lift of blade 2 (ψ=90°) has completely fallen down at the tip, while its level is rather high at the root. The lift of blade 3 has also largely decreased at the tip. The evolutions of the lift coefficient are also very different between the four blades, in their inner part (0.5 ≤ r/R ≤ 0.8). Then, from Vz=-5m/s, one can notice for each blade, a succession of drop of the lift at the tip, as well as the presence of a high level of lift at the root, when the descent rate is decreased.

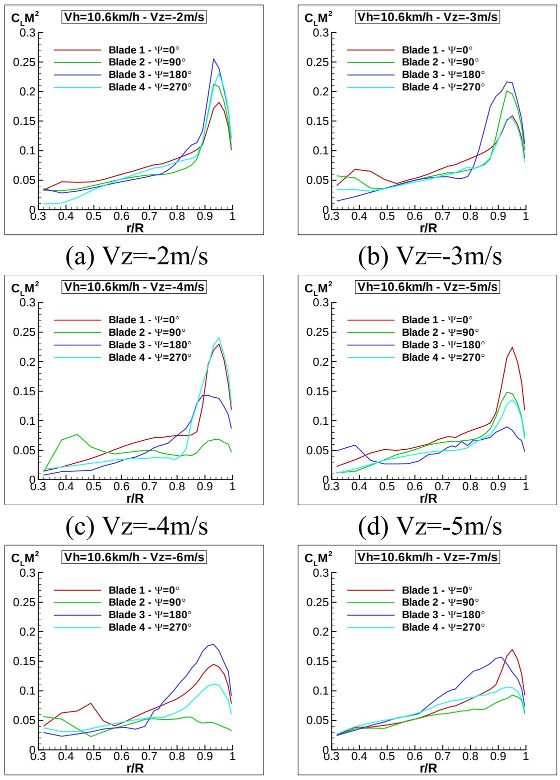

(a) Vz=-2m/s (b) Vz=-3m/s

(c) Vz=-4m/s (d) Vz=-5m/s

(e) Vz=-6m/s (f) Vz=-7m/s

Figure 12: Radial evolutions of the sectional lift coefficient for each descent rate (Vh=10.6km/h)

For the knee configuration, it can be noticed in Figure 13 that the evolutions of the sectional lift coefficient are very different between Vz=-2m/s and Vz=-3m/s, with especially the sudden drop of the lift at the tip of blades 2 and 4, and the presence of a zone of high level of lift at the root of blade 1. These evolutions can be considered as aerodynamic characteristics of entry into VRS of the helicopter. Then, for Vz=-4m/s, blade 4 presents a lifting area at its root and its tip. It has been checked that for higher descent rates, there is a succession of drop and increase of the lift for the blades, which shows the unsteady characteristic of the VRS phenomenon.

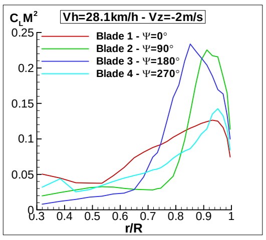

(a) Vz=-2m/s

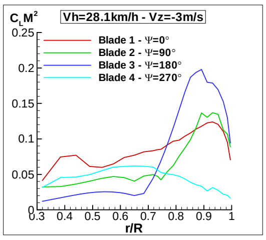

(b) Vz=-3m/s

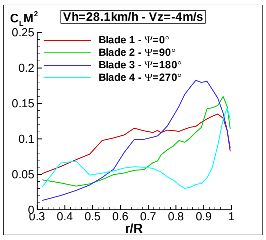

(c) Vz=-4m/s

Figure 13: Radial evolutions of the sectional lift coefficient for each descent rate (Vh=28.1km/h)

Finally, for the lower limit configuration, Figure 14 shows that for Vz=-19m/s, the evolutions of the local loads are very similar for the four blades. From Vz=-18m/s, very important differences on the local behavior of the blades can be noticed, such as a clear increase of the lift of blade 4. For blade 3, an area of increased lift appears in the inboard of the blade, with a maximum value around 0.6R. The occurrence of such sudden changes of the local loads leads to estimate the entry into VRS by the MINT calculations at Vz=-18m/s. Then from Vz=-17m/s, the loads distributions on the blades show a rapid alteration of the lift, with a succession of drop and increase phases. These changes, linked to the unsteadiness of the VRS phenomenon, are all the more important since the advancing velocity is low.

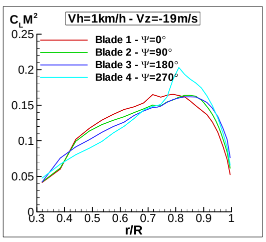

(a) Vz=-19m/s

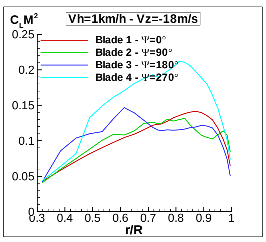

(b) Vz=-18m/s

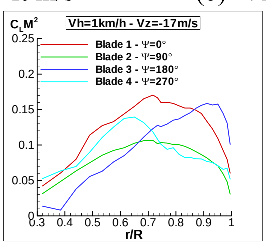

(c) Vz=-17m/s

Figure 14: Radial evolution of the sectional lift coefficient for each descent rate (Vh=1km/h)

This analysis clearly shows that the evolutions of the lift coefficient of the different blades of the rotor begin to be largely modified for a descent rate between -3 and -4 m/s for the upper limit case, at -3m/s for the knee configuration, and at -18m/s for the lower limit case. The following characteristics can be associated to the entry into VRS phenomenon:

- Drop of local lift at the blade tip;
- High level of lift at the blade root.

Normal vorticity

The evolutions of the local lift are directly linked with the evolutions of the vortices generated by the blades, during the different steps of the descent velocity. The normal vorticity fields in two cut slices, the first one perpendicular to the Y axis (containing Blades 1 and 3), and the second one perpendicular to the X axis (containing Blades 2 and 4), are analyzed respectively for the three flight cases in Figure 15.

Concerning the upper limit configuration, Figure 15 shows that for Vz=-2m/s, the generation of the tip vortices is distinct (the conservation of the 6 rotor revolutions in the wake can be clearly seen). The operating conditions of the helicopter are “classical”. The air goes through the rotor disk from top to bottom. The generation of swirly areas takes place beneath or at the level of the rotor disk plane. For Vz=-3m/s, the generation of the tip vortices is still distinct, but the envelope of the swirly areas begins to be located above the rotor disk plane (especially for blades 1 and 4). We can also notice the presence of an area of high amplitude of vorticity at the root of blade 1 (to be linked with the high level of local lift described in Figure 12). For Vz=-4m/s, the tip vortices are clustered at the tip of blades 2, 3 and 4. The envelopes of the recirculation zones become larger, and are now largely located above the rotor disk plane. These flowfield characteristics correspond to the occurrence of the entry into VRS phenomenon, described in [5]. From Vz=-5m/s, the VRS phenomenon is characterized by a succession of clustering and separation of the tip vortices (corresponding to the successive increase and decrease of the local lift at the tip shown in Figure 12), as well as the generation of large recirculation areas at the blade root (to be linked with the high values of local lift at the root shown in Figure 12). Moreover, the envelopes of the recirculation zones are maintained large and above the rotor disk plane.

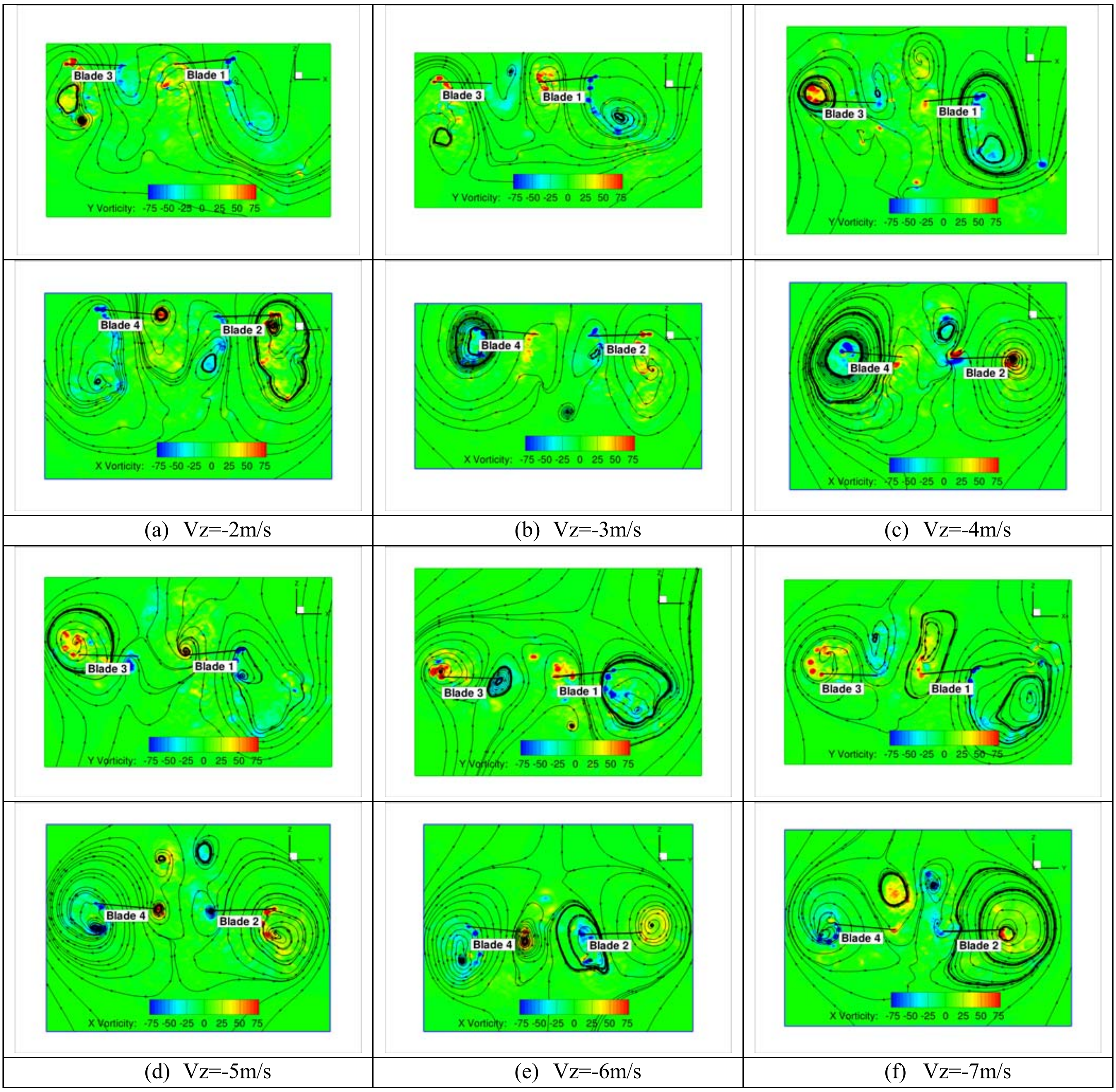

(a) Vz=-2m/s (b) Vz=-3m/s (c) Vz=-4m/s

(d) Vz=-5m/s (e) Vz=-6m/s (f) Vz=-7m/s

Figure 15: Normal vorticity fields and streamlines (Vh=10.6km/h)

Concerning the knee configuration, one can notice in Figure 16 that for Vz=-2m/s, the envelope of the recirculation zone at the tip of blade 4 is rather big. The tip vortices generated by blades 2 and 3 are clustered, which explains the high level of lift for these blades at their tip (Figure 13a). For Vz=-3m/s, the tip vortices of blade 4 are completely separated from the blade, which explains the drop of lift for this blade observed in Figure 12b. The swirly structures at the root of blade 1 are very concentrated, which explains the corresponding high level of lift in Figure 12b. For Vz=-4m/s, we can notice the generation of a recirculation area at the root of blade 1, enough intense to create lift all along the span of the blade (as observed in Figure 12c). The tip vortices of blade 4 are now attached to the blade, which explains the increase of lift at the tip of this blade (Figure 12c). The envelope of the recirculation zone at the tip of blade 2 is largely located above the rotor disk.

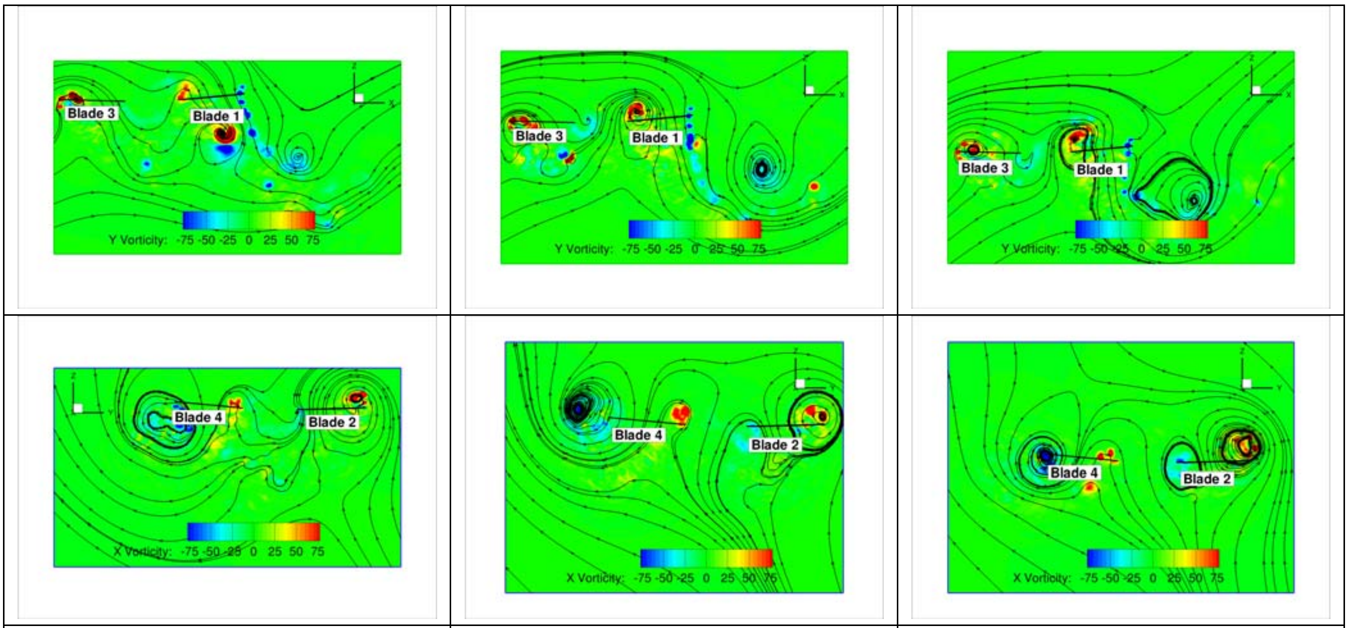

(a) Vz=-2m/s	(b) Vz=-3m/s	(c) Vz=-4m/s

Figure 16: Normal vorticity fields and streamlines (Vh=28.1km/h)

Generally speaking for the lower limit configuration (Figure 17) at this low advancing velocity, the predominant flow has the characteristics of a descent flight (streamlines in the upward direction). For Vz=-19m/s, the tip vortices generated by the blades 1, 2 and 3 are well separated one from each other. The presence of vortices generated at the root of blades 1, 3 and 4 can also be noticed. For Vz=-18m/s, the tip vortices of blade 3 are suddenly split, while those of blade 2 are clustered. All these evolutions can be considered as aerodynamic characteristics of entry into VRS. Moreover, due to the low advancing velocity, the vortices slowly move above the blades, which creates areas of high local lift in the inner part of the blades (as it is the case for blade 4). Then, from Vz=-17m/s, a succession of clustering and splitting of the root and tip vortices can be observed, which is directly linked with the rapid changes of the local lift, described in Figure 14.

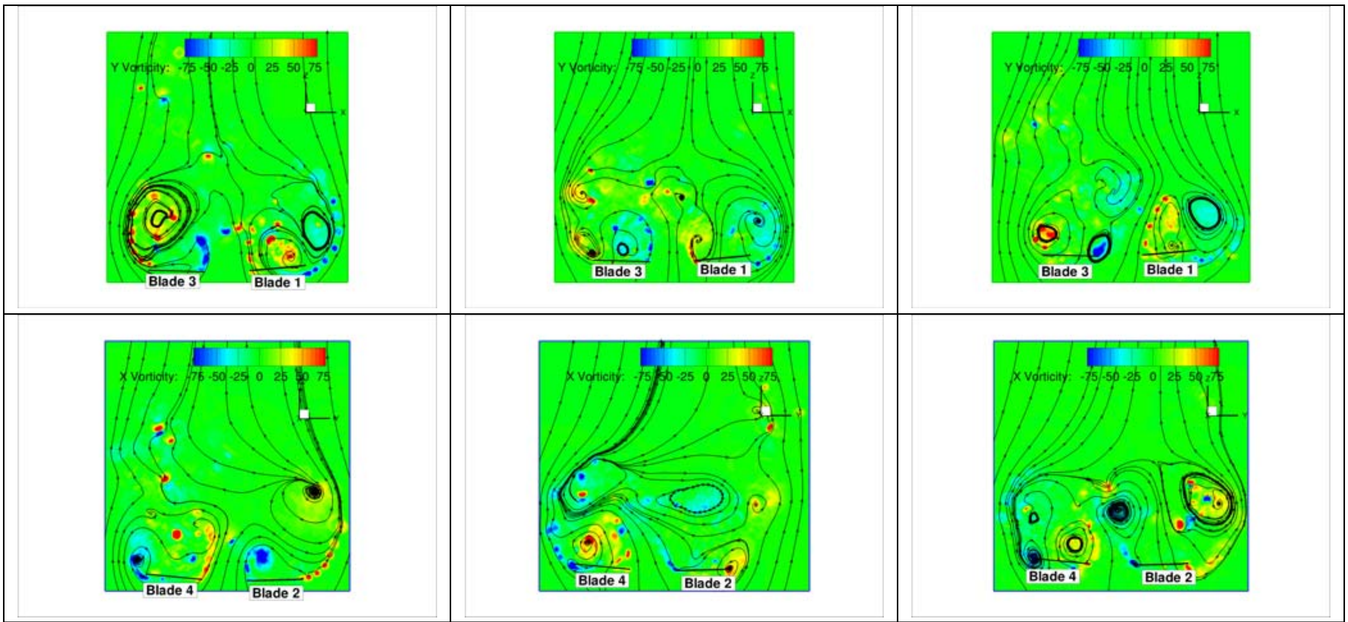

(a) Vz=-19m/s	(b) Vz=-18m/s	(c) Vz=-17m/s

Figure 17: Normal vorticity fields and streamlines (Vh=1km/h)

Q-criterion

The tri-dimensional visualizations of the iso-surfaces of the Q-criterion, for the three flight configurations, allow to qualitatively better understand the generation, the rolling up and the split of the vortices with respect to the descent rate.

Concerning the upper limit configuration, it can be shown in Figure 18 that for Vz=-2 and -3 m/s, the characteristics of the vortices are rather “classical”, the lattices being well separated one from each other. It can be noticed that the tip vortices are located above the rotor disk plane, and that areas of high intensity vorticity are present at the blade root, which explains the zones of high local lift values at the root for blades 1 and 2 (Figure 12). For Vz=-4m/s, the structure of the flowfield has drastically changed, with the roll-up of the lattices, which can be linked with the cluster of the tip vortices observed in Figure 15. Once again, these characteristics seem to be related with the entry into VRS phenomenon. From Vz=-5m/s, a succession of roll-up and split of the lattices can be observed, which can be linked the successive increase and decrease of the local lift.

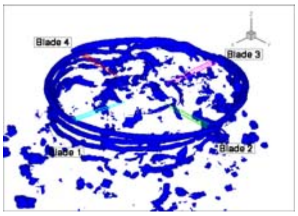
(a) Vz=-2m/s

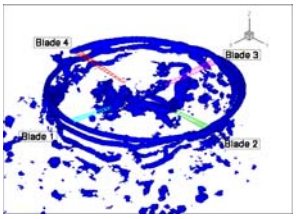
(b) Vz=-3m/s

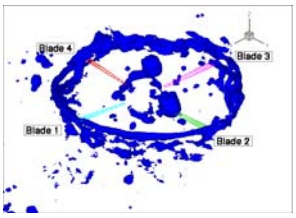
(b) Vz=-4m/s

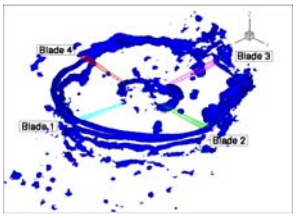
(c) Vz=-5m/s

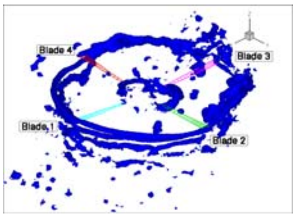
(d) Vz=-6m/s

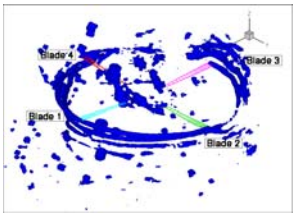
(e) Vz=-7m/s

Figure 18: Iso-surfaces of Q-criterion (Vh=10.6km/h)

Concerning the knee configuration, it can be shown in Figure 19 that for Vz=-2m/s, the roll-up of the tip vortices, especially at the rear part of the rotor disk (between blades 2, 3 and 4) is getting more intense. For Vz=-3m/s, the split of the tip vortices of blade 4 can be noticed, as well as the area of high level of vorticity at the root of blades 1, 2 and 4. For Vz=-4m/s, the tip vortices are again formed at the tip of blade 4. The tip vortices remain strongly clustered one around each other, and the vorticity area at the root of blade 1 still remains of high intensity.

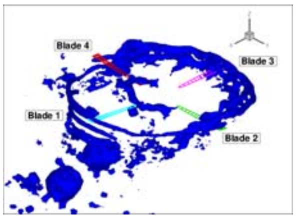
(a) Vz=-2m/s

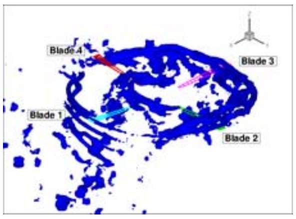
(b) Vz=-3m/s

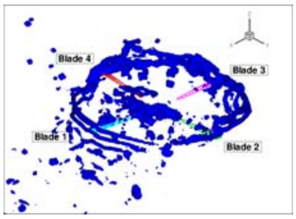
(c) Vz = -4m/s

Figure 19: Iso-surfaces of Q-criterion (Vh=28.1km/h)

Finally, for the lower limit case, Figure 20 shows that for Vz=-19m/s, the vortex lattices are clearly separated one from each other. From Vz=-18m/s, the structure of the flow is less regular, and first roll-up begin to appear, especially at the tip of blade 4. For Vz=-17m/s, the flow is clearly disorganized, the vortex lattices are strongly rolled up, and the split of the tip vortices of blade 4 can be noticed. Furthermore, an important increase of the vorticity activity can be visualized. All these characteristics are linked to the occurrence of entry into the VRS phenomenon.

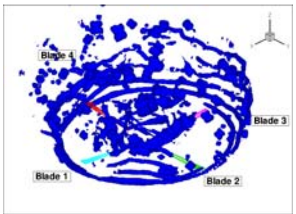
(a) Vz=-19m/s

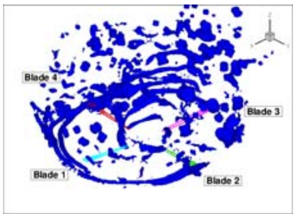
(b) Vz=-18m/s

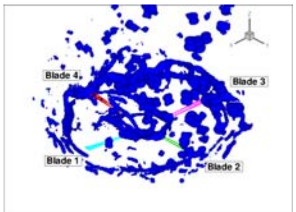
(c) Vz=-17m/s

Figure 20: Iso-surfaces of Q-criterion (Vh=1km/h)

Induced velocity

As it was previously mentioned, the VRS phenomenon occurs when the wake of the rotor cannot be "correctly" evacuated, due to the influence of the induced velocity with respect to the descent rate. The VRS criterion ε, defined in the description of the HOST code, is applied to the MINT results, and is plotted versus the descent velocity for the upper limit and the knee flight configurations, respectively in Figure 21 and Figure 22.

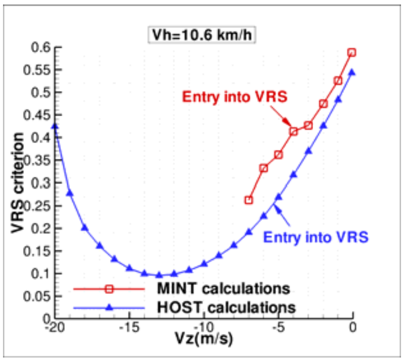

Figure 21: Comparison of the VRS criterion ε calculated for HOST and MINT results (Vh=10.6km/h)

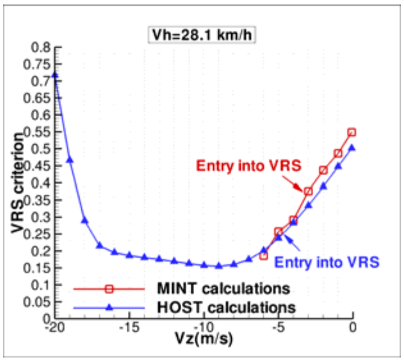

Figure 22: Comparison of the VRS criterion ε calculated for HOST and MINT results (Vh=28.1km/h)

The general evolution of the two curves is rather similar. An over-estimation of the averaged induced velocity calculated with the MINT code can be noticed with respect to the HOST results. This can explain why the descent velocity for which the VRS phenomenon is detected is lower (in absolute value) by MINT than by HOST. The entry into VRS is detected for the ε VRS criterion equal to 0.25 for the HOST code, and contained between 0.37 and 0.41 for the MINT results, depending on the flight configuration. These discrepancies are due to the different induced velocities models used in the two codes, as well as the fact that the MINT calculations are not trimmed. The values of the k and ε parameters should also be adjusted to the MINT results.

For the lower limit configuration, it has been checked that the MINT results under-estimate the averaged induced velocity in comparison with the HOST ones. This explains why the descent rate for which the entry into VRS is detected is higher for the MINT calculations than for the HOST ones.

Concluding remarks and perspectives

In the framework of the PHIDIAS project, a fully time marching unsteady wake model, developed in the MINT code by ONERA, has been validated for different flight configurations corresponding to entry into the VRS phenomenon.

The flight test results on the 6075 Dauphin were used to provide the experimental data base. Three configurations were chosen:

- upper limit: moderate advancing velocity (Vh=10.6km/h), moderate descent velocity (Vz=-4.8m/s);
- knee: high advancing velocity (Vh=28.1km/h), moderate descent velocity (Vz=-4.5m/s);
- lower limit: low advancing velocity (Vh=1km/h); high descent velocity (Vz=-15.8m/s).

The strategy of the computations consists in performing successive stabilized computations, for a given advancing velocity, by progressively increasing or decreasing the descent rate.

Initial results from the HOST comprehensive code were required as input data for the MINT calculations (such as the kinematic of the blades). Moreover, adapted developments for steep descent configurations were available on the induced velocity model, as well as a criterion of entry into VRS.

It has been shown that the MINT code is able to correctly predict the couple of velocities (Vh,Vz) for which the helicopter enters into VRS. Correlations with experimental data on the one hand, and with the HOST results on the other hand are satisfactory (knowing that the trim of the helicopter is not integrated in the MINT calculations). Depending on the flight cases, discrepancies on the estimation of the descent rate (for a given advancing velocity) vary between -0.5 and -1.5m/s.

Different characteristics of entry into VRS have been identified:

from the frequency analysis of the loads:

- increase of fluctuations of the rotor loads;

- sudden increase of the power spectral density of the rotor thrust for very low and around 4/rev frequencies;
from the aerodynamic analysis:
- sudden drop of the local lift at the blade tip;
- high lifting area at the blade root;
-clustering of the tip vortices, and presence of vortices of high intensity at the blade root.

Future works will consist in using these qualitative results to improve the flight mechanic models, as well as models describing the process of merging of tip vortices (leading to instability) [14]. Some coupled calculations between HOST and MINT will also be performed, following a given unsteady flight procedure.

References

[1] Varnes D.J., Duren R.W., Wood E.R., "*An Onboard Warning System to Prevent Hazardous "Vortex Ring State" encounters*", 26th European Rotorcraft Form, The Hague, The Netherlands, September 2000

[2] Stewart W., "*Helicopter Behavior in the Vortex-Ring Conditions*", Reports and Memoranda n°3117, British Aircraft Establishment, November 1951

[3] Castles W., gray R., "*Empirical Relation Between Induced Velocity, Thrust and Rate of Descent of a Helicopter Rotor as Determined by Wind Tunnel Test on Four Model Rotors*", Technical Note n° 2474, NACA, 1951

[4] Brinson P., Ellenreider T., "*Experimental Investigation of the Vortex Ring Condition*", 24th European Rotorcraft Forum, Marseille, France, September 1998

[5] Newman S., Brown R., Perry J., Lewis S., Orchard M., Modha A., "*A Comparative Numerical Experimental Investigations of the Vortex Ring State Phenomenon in Rotorcraft*", 57th American Helicopter Society Annual Forum, Washington D.C., 2001

[6] Bonnet P., Desopper A., Heuzé D., Panafieu T., "*Dauphin 6075 Flight Test on Performance Data Analysis and Code Validation*", 24th European Rotorcraft Forum, Marseille , France, September 1998

[7] Benoit B., Dequin A.-M., Basset P.-M., Gimonet B., Von Grunhagen W., Kampa K., "*HOST, A General Helicopter Simulation Tool for Germany and France*", 56th American Helicopter Society Annual Forum, 2000

[8] Taghizad A., Jimenez J., Binet L., Heuzé D., "*Experimental and Theoretical Investigations to Develop a Model of Rotor Aerodynamics Adapted to Steep Descents*", 58th American Helicopter Society Annual Forum, Montréal, Canada, 2002

[9] Binet L., Abildgaard M., Taghizad A., von Grünhagen W., "*VRS Avoidance as Active Function on Side-Sticks*", 65th American Helicopter Society Annual Forum, Grapevine, Texas, May 2009

[10] Wolkovitch J., "*Analytical Prediction of Vortex-Ring Boundaries for Helicopters in Steep Descent*", Journal of the American Helicopter Society, vol. 17, July 1972

[11] Le Bouar-Coppens G., Costes M., Leroy-Chesneau A., Devinant P., "*Numerical Simulations of Unsteady Aerodynamics of Helicopter Rotor in Manoeuvring Flight Conditions*", Aerospace Science and Technology, vol. 8, pp. 11-25, 2004

[12] Rodriguez B., "*Numerical Simulation of Blade Vortex Interaction and Vortex Ring State Aerodynamics using a Fully Time Marching Unsteady Wake Model*", 33rd European Rotorcraft Forum, Kazan, Russia, September 2007

[13] Hoinville E., Renaud T., "*CFD Simulation of Helicopter Rotor in Vortex Ring State Regime*", 63rd American Helicopter Annual Forum, Virginia Beach, VA, May 2007

[14] Meunier P., Le Dizès S., Leweke T., « *Compte-Rendus Physique 6* » Edition Elsevier SAS, pp. 431-450, 2005

Acknowledgments

The author would like to thank Eurocopter and the Direction Générale de l'Aviation Civile (DGAC) for their funding in this study, as well as her colleagues (Laurent Binet, Benoit Rodriguez) for the technical exchanges during this study.